

Incentivising the federation: gradient-based metrics for data selection and valuation in private decentralised training

Dmitrii Usynin, Daniel Rueckert, Georgios Kaissis
 Technical University of Munich
 Munich, Germany
 Imperial College London
 London, United Kingdom

ABSTRACT

Obtaining high-quality data for collaborative training of machine learning models can be a challenging task due to A) regulatory concerns and B) a lack of data owner incentives to participate. The first issue can be addressed through the combination of distributed machine learning techniques (e.g. federated learning) and privacy enhancing technologies (PET), such as the differentially private (DP) model training. The second challenge can be addressed by rewarding the participants for giving access to data which is beneficial to the training model, which is of particular importance in federated settings, where the data is unevenly distributed. However, DP noise can adversely affect the underrepresented and the atypical (yet often informative) data samples, making it difficult to assess their usefulness. In this work, we investigate how to leverage gradient information to permit the participants of private training settings to select the data most beneficial for the jointly trained model. We assess two such methods, namely variance of gradients (VoG) and the privacy loss-input susceptibility score (PLIS). We show that these techniques can provide the federated clients with tools for principled data selection even in stricter privacy settings.

KEYWORDS

differential privacy, data valuation, federated learning

1 INTRODUCTION

To train machine learning (ML) models which are effective at solving various tasks, the model owner(s) need descriptive, diverse and well-curated training data. However, in many sensitive contexts such data (e.g. patients with rare conditions) can be very challenging to get [3, 24, 15]. Currently, various strategies can be leveraged to obtain this data defined as collaborative machine learning (CML), but these techniques still suffer from two major problems: data privacy requirements and a lack of incentive to participate.

Firstly, a number of data protection and governance regulations (such as GDPR) stipulate that the collection and usage

of sensitive data should be minimised. One solution to this problem was proposed in [21], namely federated learning (FL). However, FL on its own fails to account for the adversarial actors in collaborative settings, making it vulnerable to privacy attacks [13, 28]. One method commonly used to alleviate these issues is differentially private (DP) training [10], often in the form of differentially private stochastic gradient descent (DP-SGD) [1], which is capable of providing objective and quantifiable guarantees of privacy for each client.

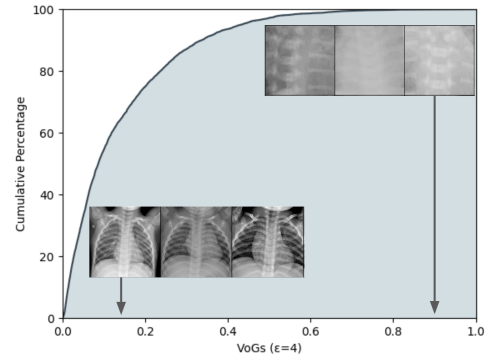


Figure 1: Distribution of normalised VoG scores for ResNet-18 (PPPD, $\epsilon=4$). Higher values indicate atypical samples.

Secondly, in order to train such models, data of high utility needs to be selected. This is often data which contains more features of interest or is scarce. However, it is often challenging to obtain access to such data samples. The problem is twofold: Currently there is no general agreement on how to establish how much individual data samples are worth and the model owners do not have the incentive to pay for them unless their model is likely to improve from it. To alleviate these issues, the relative usefulness of the data can be quantified and used to reward the participants. Many of these methods have been adapted to FL, permitting analysis of the values associated with individual data points without

needing to inspect the underlying data, such as [32] or [2], which can help model owners to guide the training process and reward the participants appropriately.

While both of these problems can be reasonably alleviated individually, addressing both of them simultaneously can be challenging. DP often affects the utility of the resulting model [5], rendering many training analysis techniques infeasible. And as a result, it can be challenging to objectively assess the contributions of each individual participant. Therefore, many commonly employed data attribution techniques, such as per-sample loss values or gradient norms [4, 22] often fail to objectively assess the individual contributions in DP settings. Additionally, DP training was shown to result in biased models, which perform worse on underrepresented subgroups [11], further reducing the diversity of the shared contributions. Methods such as data valuation using Shapley Values [18, 27] can often be rendered ineffective due to gradient clipping, reducing the contributions for diverse and out-of-distribution (OOD) samples [17]. Moreover, as computational performance can be critical in many collaborative settings, DP training itself can add a significant performance overhead. As a result, methods such as leave-one-out (LOO) [17], which requires retraining the model multiple times or calculation of Shapley values can be too costly to employ.

In this work we identify a number of methods which can be used to select “useful” training samples for both normal and DP training. While there exists a number of definitions of sample usefulness, in this work we refer to samples, which, upon exclusion from the dataset, lead to poorer model generalisation (similarly to the definition of [6]). One method to achieve this is the Variance of Gradients (VoG) [2], which allows the participants to evaluate the difficulty of individual data samples, and select data points that are more challenging for the model to learn from (we demonstrate a range of such samples in Figure 1) and can, thus, benefit generalisation. In this work, the notions of image *difficulty* and *atypicality* are used identically to [2]. To improve training data diversity, we employ the the privacy loss-input susceptibility (PLIS) [25] score. Typically, this metric is used to identify more privacy-sensitive (we also refer to them as *revealing* in this work) attributes and data points, however, it has also previously been used to detect atypical/OOD samples in sensitive datasets and is explicitly formulated for DP training. Both of these metrics can also be conveniently realised as easily comparable scalar values. This, in turn, simplifies the identification of more valuable samples and a reward allocation process. Through extensive experimental results we show that these metrics can be used to augment the existing FL settings with both privacy and incentivisation in mind.

Overall, the contributions of this work can be summarised as follows:

- We investigate how gradient-based metrics can be used in collaborative DP machine learning to identify samples of higher utility and compare them to commonly used sample utility metrics
- We provide initial evidence that gradient-based metrics can be used to effectively identify samples of interest in DP and non-DP settings across a variety of model architectures, datasets and privacy regimes
- As these metrics are themselves privacy-sensitive, we propose a DP version of these metrics that can be shared with other participants. This allows the federation to identify sites with non-standard datasets and individuals, who can be reimbursed for access to their data

2 BACKGROUND AND RELATED WORK

2.1 Differential privacy

There exists a large number of works on PETs deployed in low-trust collaborative environments [29]. In this work we are specifically interested in a method which would allow the federation to retain their *output* privacy [30], which entails protection of their sensitive data (and its derivatives) from adversaries who are part of the training consortium or are able to query the model that has already been trained. As the the definition of *input* privacy has already been satisfied through the use of FL, we, thus study the concept of differential privacy used to ascertain the privacy of the information stored in the shared model updates.

Definition 2.1 ((ϵ, δ)-DP, [10]). We say that the randomised mechanism \mathcal{M} preserves (ϵ, δ)-DP if, for all pairs of adjacent databases D and D' and all subsets \mathcal{S} of \mathcal{M} 's range:

$$\mathbb{P}(\mathcal{M}(D) \in \mathcal{S}) \leq e^\epsilon \mathbb{P}(\mathcal{M}(D') \in \mathcal{S}) + \delta. \quad (1)$$

Most properties of (ϵ, δ)-DP are described in detail in [10]. In simple terms, the output of a DP algorithm is approximately invariant to an inclusion or an exclusion of an individual.

2.2 Data valuation

In this work we are interested in determining the importance or value of individual data points. Most prior works in this area rely on the aforementioned Shapley values or LOO retraining in order to determine the usefulness of the shared data [17, 14, 26]. However, as our setting employs DP, some of the data, particularly the outliers, can be adversely affected by gradient noise when approximating the importance of individual data points [7, 11]. Additionally, these calculations are very computationally expensive, resulting in large overhead during training, which can render these methods infeasible in many settings.

3 METHODS

In this work we employ the variance of gradients method described in [2]. Formally, pixelwise VoG_p is defined as follows:

$$\text{VoG}_p = \sqrt{\frac{1}{K} \sum_{t=1}^K (S_t - \mu)^2}, \quad (2)$$

where $\mu = \frac{1}{K} \sum_{t=1}^K S_t$, K denotes time steps, N denotes input pixels and S_t is the gradient of the loss with respect to the input pixels. The scalar VoG is calculated from the averaged pixel-wise variance of gradients over all time steps as $\frac{1}{N} \sum_{t=1}^N (\text{VoG}_p)$. Similarly to [2], we perform per-class normalisation. However, unlike [2], we normalise the values to lie in the region of [0, 1] for easier interpretability.

Additionally, we also employ PLIS [25], which is defined as follows:

$$\begin{aligned} \text{PLIS}(S_i) &:= J_{x_i}(\text{PL}(S_i)) \\ &= J_{x_i} \left(\frac{\|\nabla_{\theta} \ell(x_i|y_i, \theta)\|_2^2}{\sigma^2} \right). \end{aligned} \quad (3)$$

Where $\text{PL}(S_i)$ is:

$$\text{PL}(S_i) \propto \frac{\|\nabla_{\theta} \ell(x_i|y_i, \theta)\|_2^2}{\sigma^2}. \quad (4)$$

Here J_{x_i} is a Jacobian with respect to the input attribute i ; $\ell(f(x, \theta), y)$ is the loss function of a neural network $f(x, \theta)$, where (x_i, y_i) is a input/label pair belonging to subject S_i , and θ is a vector of learnable parameters

In this work we report the spectral norm (L_2 -norm) of the PLIS matrix, which allows the individuals to utilise a single scalar value to approximate their privacy-loss with the respect to the input features. We normalise the class-wise PLIS scores to lie in the region of [0, 1] for easier interpretability.

We provide the descriptions of our training settings, including models and datasets used, hardware and privacy regimes in Appendix A.1.

4 RESULTS AND DISCUSSION

We find that, in general, the selected images between the DP and non-DP settings are very similar (Figure 2). In both settings, the samples selected are atypical and represent the data that can be considered difficult for a model to learn from. We now discuss how VoG and PLIS values can be affected in different learning settings and how they compare against other commonly used metrics.

Our main findings can be summarised as follows:

- Unlike most of the commonly used techniques, VoG-based sample selection is consistent across many model architectures, datasets and privacy regimes;

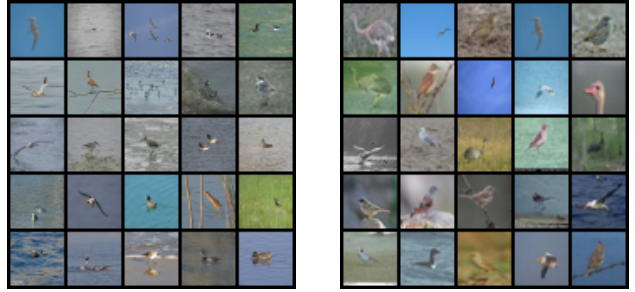


Figure 2: Comparison of images with largest VoGs for WideResNet-50 ($\epsilon=4$) and ResNet-101 ($\epsilon=4$) respectively (CIFAR-10, *bird* class). The trend for low contrast and more defined features is maintained across different model architectures (SSIM of 0.552 and BD of 0.698).

- Larger models are, in general, more difficult to analyse, as the sample selection is not consistent for larger datasets;
- While both PLIS and VoG scores can be utilised to identify samples of interest, they account for different information content and can be used to prioritise different sample types.

We quantify the selection “consistency”, using the structural similarity index (SSIM) [31] and the Bhattacharyya distance (BD) [19] between the pixel distributions of the images. Higher SSIM and lower BD distance indicate similar images. Alternative metrics can be employed instead (e.g. the Fretchet Inception distance [16]).

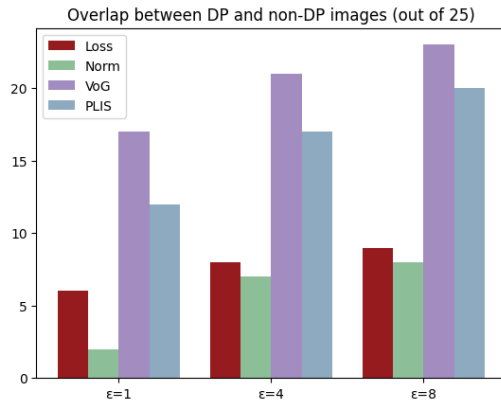


Figure 3: Comparison between different selection methods under normal and DP training (ResNet-18, CIFAR-10). Higher is better.

4.1 Comparing against per-sample losses and gradient norms

We firstly compare the metrics we selected against the commonly used sample selection strategies in FL: per-sample loss and L_2 -gradient norm values. Both of these are often used as proxies for estimation of sample difficulty in FL [4, 22, 23, 33]. However, due to the addition of noise and aggressive gradient clipping, the selected images are not consistent in DP settings (exemplified in Figure 3). We notice that there is a large amount of variation between the images in the private and non-private settings (Figure 4), and in some cases there is almost no overlap between the two. The Pearson correlation coefficients of the top 1000 private ($\epsilon = 4$) and non-private scores were 0.09 and 0.18 (loss values and gradient norms respectively). In comparison (discussed below), both the VoG and PLIS scores are consistent across most models, datasets and privacy levels. Therefore, while loss- and norm-based metrics can identify similar images compared to VoG and PLIS scores in non-private settings, they are not suitable for DP training.

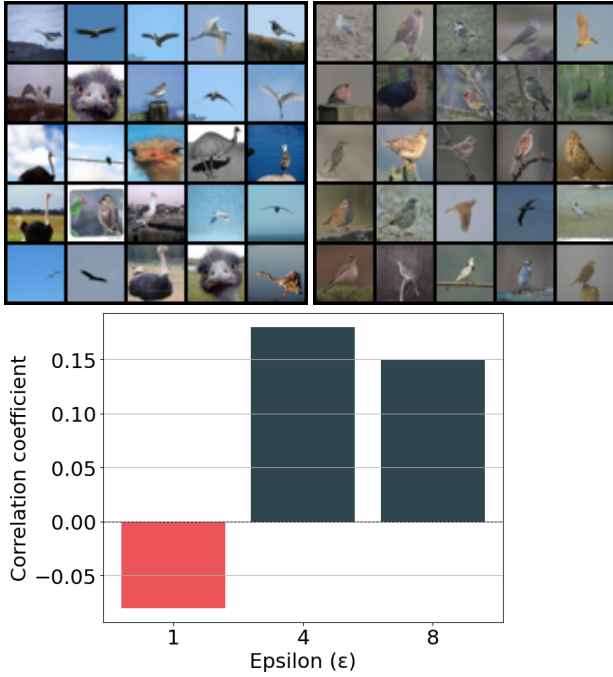


Figure 4: Comparison of images with largest gradient norms for DP and non-DP models respectively (ResNet-18, CIFAR-10, bird class, $\epsilon = 4$). There is little conceptual similarity between the chosen images (low correlation coefficients at different ϵ values, the SSIM of 0.355 and the BD of 0.914).

4.2 Increasing the model size

We observe that, in general, regardless of the number of parameters (and of the architecture) the VoG scores can be used to successfully identify the atypical samples in lower-dimensional datasets (Figure 2). However, we also notice that larger models tend to be more challenging to analyse. We show exemplary results in Figure 5 and note that there is a significant difference between the images of interest for ResNet-18 and ResNeXt-101 for both the DP and non-DP models. We notice that as the model size grows, for PPPD the usefulness of each individual sample becomes more difficult to define and the selected images feature both highly-detailed X-rays as well as blurry images with an undersized field of view. This could make the adoption of VoG-based methods trickier for settings that employ models with a larger number of parameters. To summarise: We tend to see very consistent sample selection for smaller images, but for larger images, the attribution is more challenging to interpret.

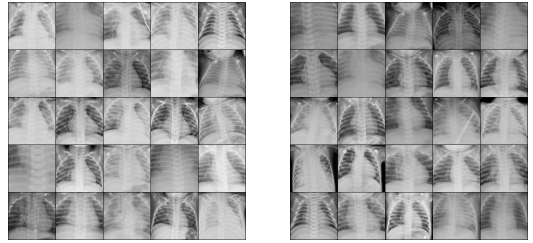


Figure 5: Comparison of images with largest VoGs for ResNet-18 and ResNeXt-101 respectively (non-private models PPPD). Here there is some variation in the images (SSIM of 0.521 and BD of 0.320) based on the size of the model even in non-private settings.

4.3 Effects of changing the ϵ -value

We discovered that the atypical images identified with VoG scores are consistent across all privacy levels for lower-dimensional datasets, showing that participants can effectively employ VoGs for sample selection with strong privacy guarantees. We show exemplary results in Figure 6, where the images selected across all privacy levels are almost identical (with SSIM being close to 1.0). However, for PPPD, we observe that there is more variation in image selection. We note that the trend of atypical images being considered to be more difficult remains the same, but the features which make these images stand out differ. We show these results in Figure 7 and hypothesize that there could be two factors at play here. Firstly, the size and the complexity of the dataset, which we discuss in detail below. Secondly, the accuracy of the model: For smaller images, the accuracy of the trained model does not seem to have an impact in private settings,

but for PPPD (e.g. the accuracy difference between ϵ of 1 and 8 on ResNet-18 is 21.1%) the results vary severely. One interesting discovery is that for a lower value of ϵ , the selected images seem to be more atypical, showing that models of lower accuracies could be used to identify images, which a human observer would also consider to be more unusual. We hypothesise that this might be due to the fact that a more private model might only concentrate on the “core” image features.

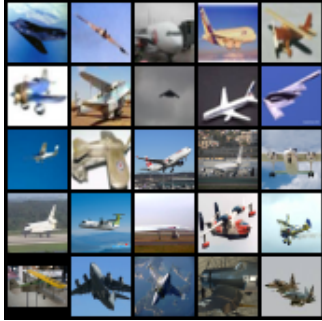


Figure 6: Images with largest VoGs for ϵ of 1 and 8 (ResNet-18, CIFAR-10, *airplane* class). Selected samples are identical with an SSIM of 1.0.

A similar observation can be made about the relationship between the value of ϵ and the samples of interest detected using the PLIS score. In moderate-to-low noise settings (ϵ of 4 and 8 respectively), most privacy-sensitive samples remain fairly consistent (with SSIMs in a range of 0.8). However, for ϵ of 1, we observe a very different set of selected images. This could have a similar implication of the model only concentrating on the most revealing features of the input image, or be due to an over-proportional decrease in memorisation ability at low privacy values, as discussed in [12]. As part of future work, these results could help us find the answer to a more fundamental question: “If a model is restricted to only learning from a small subset of features, which features would it learn first?”

4.4 Changing the dataset

Both the small and the large image settings showed that VoGs could be successfully leveraged to identify atypical samples across all values of ϵ regardless of the dataset. We note that PPPD showed more variation of samples of interest across different model architectures and ϵ values. We hypothesise that this can be the case either due to A) PPPD much smaller (only 5 400 samples), or B) only containing a single input channel, resulting in a more profound role of the contrast of the image. Thus, we see that regardless of the quality of the individual samples, the higher values identify images which show lower contrast and level of detail. We show exemplary

results for the largest and the smallest VoGs for PPPD in Figure 7. Finally we note, that as the dataset size grows (e.g. comparing CIFAR-10 and CINIC-10), the selection consistency grows as well with 21 and 24 overlapping samples (out of 25) for $\epsilon=4$ respectively. We show exemplary results in Figure 8.

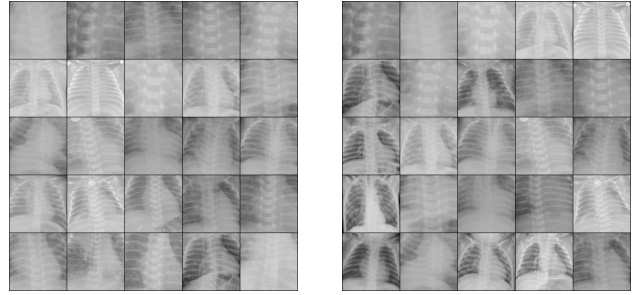


Figure 7: Comparison of images with largest VoGs for ϵ of 1 and 8 respectively (ResNet-18, PPPD). The overall selection criteria (low contrast and unclear anatomical details) remains consistent (SSIM of 0.722 and BD of 0.074).

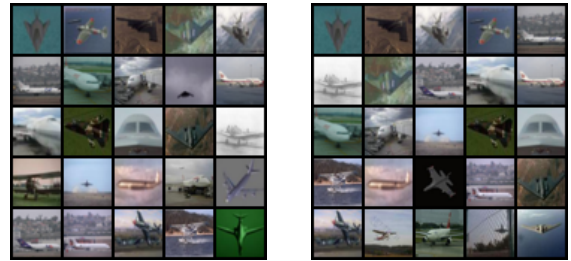


Figure 8: Comparison of images with largest VoGs for ϵ value of 4 and 8 respectively (ResNet-9, CIFAR-10, *airplane* class). 21/25 images are identical.

4.5 Relationship between PLIS and VoGs

When comparing the PLIS and VoG scores, we notice that there no immediate correlation between them (0.57 and 0.55 values of Pearson correlation coefficient respectively). In Figure 9, we see that some images, which we would expect to have large VoG scores (i.e. those that are less clear visually) posses the smallest PLIS values, meaning that the selection for images with particularly large/small VoG and PLIS could often be contradictory (0.33 and 0.34 values of Pearson correlation coefficient respectively). Furthermore, we see in Figure 10 that the images with lowest PLIS scores are not consistent across DP and non-DP settings. This may suggest that while PLIS could be used to identify atypical images, it is unlikely

to be consistent in identifying more difficult data samples when performing DP and non-DP training.

This raises an interesting issue: Images with high PLIS values are considered to have more revealing features and images with high VoG are considered to be difficult for the model to learn from. Intuitively, one would expect that more revealing features would correspond to rare, OOD samples [25], making these features more uniquely identifying. However, when comparing their PLIS and VoG values, we see that the model does not necessarily see them as more “challenging” to learn from. One reason behind this might be that, similarly to [35], revealing features should correspond to more informative samples, as they contain more useful features for the model to learn from (and are considered to be *easier*). And, as a result, high PLIS may indicate that the sample has rare features, which are easy for the model to learn from. An in-depth investigation of “what makes a sample informative” and how it correlates to its difficulty is part of our ongoing work in this area.

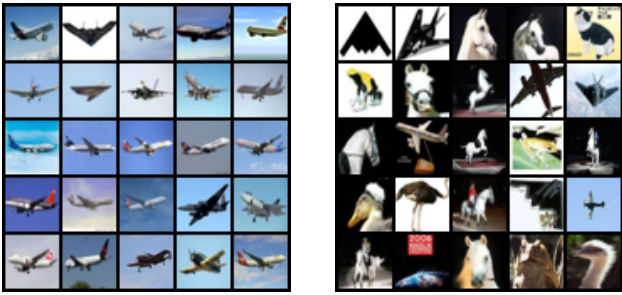


Figure 9: Images with the smallest VoG and PLIS scores respectively (ResNet-18, $\epsilon = 1$, CIFAR-10). The selection of images is severely different based on which metric is used (SSIM of 0.215 and BD of 0.886).

4.6 Importance sampling for model training

In addition to incentivisation of the data owners, many of these metrics are often used for sample selection in decentralised model training, pruning the training set over time to remove redundancy and decrease training time. We simulated such scenarios by training the model for 5 to 10 epochs depending on the complexity of the task and then removing a proportion (between 0.25 and 0.35) of the dataset based on the metrics of interest. The training then resumes (for 10-20 epochs based on the complexity of the task). We show our preliminary results in Table 1 and reduce the overall training time by 50%. Here we observe two distinct results when removing the most difficult samples (i.e those with the highest metrics). Firstly, for all metrics the train-time

accuracy increases (and in most cases gets close to 100% in non-private settings). Secondly, for loss- and gradient-norm-based removal, the resulting test-time accuracy was on average much higher compared to PLIS and VoG-guided sample removal (across all ϵ levels). These results suggest that while *some* information is lost by removing the samples identified as the more difficult ones through per-sample loss and gradient norm, these samples were, in fact, not the most informative ones. On another hand, for PLIS and VoG-based removal, there was a significant drop in test-time accuracy across all privacy levels. Therefore, we hypothesise that the difficulty captured through VoG and PLIS values is the so-called “useful difficulty”, where highest-ranking samples are beneficial for model generalisation. Exploration of this phenomenon and its implications are part of our ongoing work in this domain.

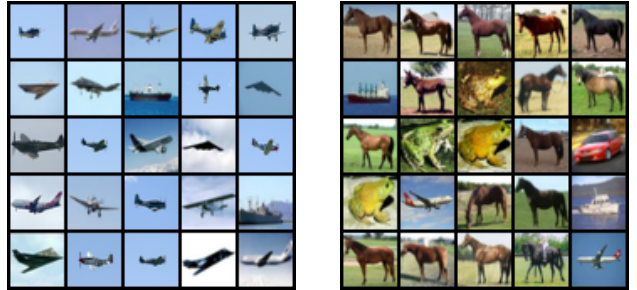


Figure 10: Comparison of images with smallest PLIS for private ($\epsilon = 4$) and non-private settings respectively (ResNet-18, CIFAR-10, all classes). The dominant classes are different.

4.7 Differentially private VoG and PLIS

As both the VoG and the PLIS values are sensitive, data-dependent quantities, these should not be published “in the clear”, as this can permit adversarial actors to identify potential victims (e.g. prioritising attacking high-valued participants). One privacy-preserving alternative would be DP publication of these values. For VoG values, we can perform differentially private variance queries ($\epsilon, 0$) and for PLIS values we propose to use clipping and use a Laplace mechanism (also $\epsilon, 0$). These steps can then either be composed (heterogeneously) with the Gaussian Mechanism used for DP-SGD training, for instance using [36], or have their own separate accountant.

5 LIMITATIONS AND FUTURE WORK

The main challenge of interpretation of these scores is the fact that not every difficult image is informative (and hence beneficial for the joint model). While our preliminary results

	Loss values	Gradient norms	VoG	PLIS
Test-time accuracy $\epsilon=1$ (%)	56.6	55.1	52.4	49.9
Test-time accuracy $\epsilon=4$ (%)	63.6	61.8	58.8	55.6
Test-time accuracy $\epsilon=8$ (%)	66.7	64.8	61.7	58.0

Table 1: Removal of 25% of all samples with highest metrics (ResNet-18, CIFAR-10).

suggest that VoG and PLIS scores tend to favor more useful samples, further work is needed to identify which features make a sample difficult and/or informative.

As we outlined in Section 4.7, both the VoG and the PLIS values are sensitive, as they are derived directly from the private characteristics of the model. Therefore, these should only be shared in a privatised form, which could reduce their descriptiveness in settings with lower values of ϵ . This could lead to misalignment of the *usefulness* of the data and the associated rewards. The investigation of which specific input features contribute towards higher “useful difficulty” of the sample is a promising area of future research. Investigation of the relationship between these metrics and model memorisation [12], is part of our ongoing work. Additionally, when studying the effects of federated retraining, extra care is required when calculating the privacy guarantees for the retrained model. This is because both the sampling rates as well as the individuals in the dataset who benefit from the guarantees are directly affected.

As both the VoG and PLIS (and even the L_2 -norm) calculations heavily rely on per-sample gradients, these methods are computationally limited by the speed of this calculation. We see a noticeable overhead in performance, in some cases almost doubling the training time of the original model. Therefore, gradient-based metrics can perform best in settings where dataset pruning results in a larger gain in performance than the computational overhead of these methods, as these metrics need to only be calculated once. Our preliminary retraining results show that notable performance improvement can already be achieved using these metrics for data selection and we aim to continue this investigation in large-scale federated settings as part of the future work.

6 CONCLUSION

In this work, we show that it is possible to employ gradient-based metrics to identify samples of interest in private collaborative image analysis tasks. We show that these can be effectively used to augment the FL imaging settings to permit more effective data selection. These methods are economical computationally, effective across a range of different computer vision tasks on a variety of model architectures

and perform well even in low-trust environments. We note that VoG, while not originally designed with private training in mind, can be effectively used to identify such samples irrespective of the desired privacy level for a range of ϵ in many learning settings. While PLIS was originally specifically developed to serve DP model training, we found that it could be less consistent when compared to VoG-based data selection depending on the value of ϵ . A direct comparison between these two values shows that it is very challenging to precisely define the notion of a difficult and informative sample. We hope that this work would encourage researchers to study the question of private-preserving data valuation further, encouraging further scientific collaboration and wider adoption of safe FL.

REFERENCES

- [1] Martin Abadi, Andy Chu, Ian Goodfellow, H Brendan McMahan, Ilya Mironov, Kunal Talwar, and Li Zhang. 2016. Deep learning with differential privacy. In *Proceedings of the 2016 ACM SIGSAC conference on computer and communications security*, 308–318.
- [2] Chirag Agarwal, Daniel D’souza, and Sara Hooker. 2022. Estimating example difficulty using variance of gradients. In *Proceedings of the IEEE/CVF Conference on Computer Vision and Pattern Recognition*, 10368–10378.
- [3] Muhammad Aurangzeb Ahmad, Arpit Patel, Carly Eckert, Vikas Kumar, and Ankur Teredesai. 2020. Fairness in machine learning for healthcare. In *Proceedings of the 26th ACM SIGKDD International Conference on Knowledge Discovery & Data Mining*, 3529–3530.
- [4] Mohammad Mohammadi Amiri, Deniz Gündüz, Sanjeev R Kulkarini, and H Vincent Poor. 2021. Convergence of update aware device scheduling for federated learning at the wireless edge. *IEEE Transactions on Wireless Communications*, 20, 6, 3643–3658.
- [5] Eugene Bagdasaryan, Omid Poursaeed, and Vitaly Shmatikov. 2019. Differential privacy has disparate impact on model accuracy. *Advances in neural information processing systems*, 32.
- [6] Robert Baldock, Hartmut Maennel, and Behnam Neyshabur. 2021. Deep learning through the lens of example difficulty. *Advances in Neural Information Processing Systems*, 34, 10876–10889.
- [7] Xiangyi Chen, Steven Z Wu, and Mingyi Hong. 2020. Understanding gradient clipping in private sgd: a geometric perspective. *Advances in Neural Information Processing Systems*, 33, 13773–13782.
- [8] Luke N Darlow, Elliot J Crowley, Antreas Antoniou, and Amos J Storkey. 2018. Cinc-10 is not imagenet or cifar-10. *arXiv preprint arXiv:1810.03505*.
- [9] Soham De, Leonard Berrada, Jamie Hayes, Samuel L Smith, and Borja Balle. 2022. Unlocking high-accuracy differentially private image classification through scale. *arXiv preprint arXiv:2204.13650*.

- [10] Cynthia Dwork and Aaron Roth. 2014. The algorithmic foundations of differential privacy. *Foundations and Trends® in Theoretical Computer Science*, 9, 3–4, 211–407. DOI: 10.1561/04000000042.
- [11] Tom Farrand, Fatemehsadat Miresghallah, Sahib Singh, and Andrew Trask. 2020. Neither private nor fair: impact of data imbalance on utility and fairness in differential privacy. In *Proceedings of the 2020 workshop on privacy-preserving machine learning in practice*, 15–19.
- [12] Vitaly Feldman. 2020. Does learning require memorization? a short tale about a long tail. In *Proceedings of the 52nd Annual ACM SIGACT Symposium on Theory of Computing*, 954–959.
- [13] Jonas Geiping, Hartmut Bauermeister, Hannah Dröge, and Michael Moeller. 2020. Inverting gradients—how easy is it to break privacy in federated learning? *arXiv preprint arXiv:2003.14053*.
- [14] Amirata Ghorbani and James Zou. 2019. Data shapley: equitable valuation of data for machine learning. In *International conference on machine learning*. PMLR, 2242–2251.
- [15] Ben Glocker, Charles Jones, Mélanie Bernhardt, and Stefan Winzeck. 2023. Algorithmic encoding of protected characteristics in chest x-ray disease detection models. *Ebiomedicine*, 89.
- [16] Martin Heusel, Hubert Ramsauer, Thomas Unterthiner, Bernhard Nessler, and Sepp Hochreiter. 2017. Gans trained by a two time-scale update rule converge to a local nash equilibrium. *Advances in neural information processing systems*, 30.
- [17] Ruoxi Jia, Fan Wu, Xuehui Sun, Jiace Xu, David Dao, Bhavya Kaillkhura, Ce Zhang, Bo Li, and Dawn Song. 2021. Scalability vs. utility: do we have to sacrifice one for the other in data importance quantification? In *Proceedings of the IEEE/CVF Conference on Computer Vision and Pattern Recognition*.
- [18] Ruoxi Jia et al. 2019. Towards efficient data valuation based on the shapley value. In *The 22nd International Conference on Artificial Intelligence and Statistics*. PMLR, 1167–1176.
- [19] Thomas Kailath. 1967. The divergence and bhattacharyya distance measures in signal selection. *IEEE transactions on communication technology*, 15, 1, 52–60.
- [20] Georgios Kaissis et al. 2021. End-to-end privacy preserving deep learning on multi-institutional medical imaging. *Nature Machine Intelligence*, 3, 6, 473–484.
- [21] Jakub Konečný, H Brendan McMahan, Felix X Yu, Peter Richtárik, Ananda Theertha Suresh, and Dave Bacon. 2016. Federated learning: strategies for improving communication efficiency. *arXiv preprint arXiv:1610.05492*.
- [22] Fan Lai, Xiangfeng Zhu, Harsha V Madhyastha, and Mosharaf Chowdhury. 2021. Oort: efficient federated learning via guided participant selection. In *15th {USENIX} Symposium on Operating Systems Design and Implementation ({OSDI} 21)*, 19–35.
- [23] Anran Li, Lan Zhang, Juntao Tan, Yaxuan Qin, Junhao Wang, and Xiang-Yang Li. 2021. Sample-level data selection for federated learning. In *IEEE INFOCOM 2021-IEEE Conference on Computer Communications*. IEEE, 1–10.
- [24] Vishwali Mhasawade, Yuan Zhao, and Rumi Chunara. 2021. Machine learning and algorithmic fairness in public and population health. *Nature Machine Intelligence*, 3, 8, 659–666.
- [25] Tamara T Mueller, Stefan Kolek, Friederike Jungmann, Alexander Ziller, Dmitrii Usynin, Moritz Knolle, Daniel Rueckert, and Georgios Kaissis. 2022. How do input attributes impact the privacy loss in differential privacy? *arXiv preprint arXiv:2211.10173*.
- [26] Seyedamir Shobeiri and Mojtaba Aajami. 2022. Shapley value is an equitable metric for data valuation. *Iraqi Journal for Electrical And Electronic Engineering*, 18, 2.
- [27] Rachael Hwee Ling Sim, Yehong Zhang, Mun Choon Chan, and Bryan Kian Hsiang Low. 2020. Collaborative machine learning with incentive-aware model rewards. In *International Conference on Machine Learning*. PMLR, 8927–8936.
- [28] Dmitrii Usynin, Daniel Rueckert, and Georgios Kaissis. 2022. Beyond gradients: exploiting adversarial priors in model inversion attacks. *arXiv preprint arXiv:2203.00481*.
- [29] Dmitrii Usynin, Alexander Ziller, Marcus Makowski, Rickmer Braren, Daniel Rueckert, Ben Glocker, Georgios Kaissis, and Jonathan Passerat-Palmbach. 2021. Adversarial interference and its mitigations in privacy-preserving collaborative machine learning. *Nature Machine Intelligence*, 3, 9, 749–758.
- [30] Dmitrii Usynin, Alexander Ziller, Daniel Rueckert, Jonathan Passerat-Palmbach, and Georgios Kaissis. 2021. Distributed machine learning and the semblance of trust. *arXiv preprint arXiv:2112.11040*.
- [31] Zhou Wang, Alan C Bovik, Hamid R Sheikh, and Eero P Simoncelli. 2004. Image quality assessment: from error visibility to structural similarity. *IEEE transactions on image processing*, 13, 4, 600–612.
- [32] Xinyi Xu, Lingjuan Lyu, Xingjun Ma, Chenglin Miao, Chuan Sheng Foo, and Bryan Kian Hsiang Low. 2021. Gradient driven rewards to guarantee fairness in collaborative machine learning. *Advances in Neural Information Processing Systems*, 34, 16104–16117.
- [33] Yihao Xue, Chaoyue Niu, Zhenzhe Zheng, Shaojie Tang, Chengfei Lyu, Fan Wu, and Guihai Chen. 2021. Toward understanding the influence of individual clients in federated learning. In *Proceedings of the AAAI Conference on Artificial Intelligence* number 12. Vol. 35, 10560–10567.
- [34] Ashkan Yousefpour et al. 2021. Opacus: user-friendly differential privacy library in pytorch. *arXiv preprint arXiv:2109.12298*.
- [35] Yuheng Zhang, Ruoxi Jia, Hengzhi Pei, Wenxiao Wang, Bo Li, and Dawn Song. 2020. The secret revealer: generative model-inversion attacks against deep neural networks. In *Proceedings of the IEEE/CVF Conference on Computer Vision and Pattern Recognition*, 253–261.
- [36] Yuqing Zhu, Jinshuo Dong, and Yu-Xiang Wang. 2022. Optimal accounting of differential privacy via characteristic function. In *International Conference on Artificial Intelligence and Statistics*. PMLR, 4782–4817.

A APPENDIX

A.1 Models and datasets

Here we briefly outline the model architectures and datasets used in our study. We experiment with a number of ResNet-derived architectures, namely ResNet-9, 18 as the *smaller* shared models and ResNet-101, ResNeXt-101 and WideResNet-50, 101 as the *larger* models. We use the ResNet model family, as it was previously shown to be more robust to clipping (required for DP-SGD) and has obtained very adequate accuracy in the past on a variety of computer vision tasks in both the private and the non-private training settings [9].

In this work we employ the commonly used CIFAR-10 dataset as well as two more complex tasks, namely the CINIC-10 [8] and the paediatric pneumonia prediction (PPPD) (adapted from [20]) datasets. Both CIFAR-10 (50 000 of 32x32 training images) and CINIC-10 (90 000 of 32x32 training images) are classification tasks with 10 classes. PPPD (5 400 of 224x224 training images) is a classification task with 3 classes: no pathology, bacterial pneumonia and viral pneumonia.

A.2 Experimental settings

We perform model training using PyTorch 1.13, DP training using opacus 1.3.0 [34] on two Linux 22.04 machines using NVIDIA RTX A6 000 and NVIDIA Quadro RTX 5 000 GPUs

respectively. To obtain fast per-sample gradients we employ the functorch 1.13.1 library. For differentially private training we use three distinct privacy settings, with ϵ values of 1, 4 and 8. Our δ values are dataset-defined with $\delta_{\text{CIFAR}} = 1e^{-5}$, $\delta_{\text{CINIC}} = 1.1e^{-6}$ and $\delta_{\text{PPD}} = 1e^{-4}$